Peripapillary Pachychoroid Syndrome

Nopasak Phasukkijwatana, PhD, MD [1,2], K Bailey Freund, MD[3,4], Rosa Dolz-Marco, MD, PhD[3,4], Mayss Al-Sheikh, MD[5,6], Pearse A Keane, MD[7], Cathy Egan, MD[7], Sandeep Randhawa, MD[8,9], Jay M Stewart, MD[10], Qingyun Liu, MD[10,11], Alex P Hunyor, MD[12,13], Allan Krieger, MD[1], Aaron Nagiel, MD, PhD[1], Robert Lalane, MD[1], Mansour Rahimi, MD[1], Won Ki Lee, MD[14], Lee Merrill Jampol, MD[15], David Sarraf, MD[1,16]

[1]Stein Eye Institute, David Geffen School of Medicine at UCLA, Los Angeles, California

[2]Department of Ophthalmology, Faculty of Medicine Siriraj Hospital, Mahidol University, Bangkok, Thailand

[3]Vitreous Retina Macula Consultants of New York, New York, NY, USA

[4]Department of Ophthalmology, New York University School of Medicine, New York, NY, USA

[5]Doheny Eye Institute, Department of Ophthalmology, David Geffen School of Medicine at UCLA, Los Angeles, CA, USA

[6]Department of Ophthalmology, University Hospital Zurich, University of Zurich, Zurich, Switzerland

[7]Moorfields Eye Hospital NHS Foundation Trust, London, London, United Kingdom.

[8]Associated Retinal Consultant, PC, Royal Oak, MI, USA

[9]Ophthalmology, Oakland University William Beaumont School of Medicine, Royal Oak, MI, USA

[10]UCSF, San Francisco, CA, USA

[11]Department of Ophthalmology, Tongliao City Hospital, Tongliao, Inner Mongolia, China

[12]Retina Associates, Chatswood, NSW, Australia

[13]Save Sight Institute, University of Sydney, Sydney, NSW, Australia

[14]Ophthalmology, Seoul St. Mary's Hospital, Catholic University of Korea, Seoul, Seoul, Korea

[15]Ophthalmology, Northwestern University Feinberg School of Medicine, Chicago, IL, USA

[16]Greater Los Angeles VA Healthcare Center, Los Angeles, CA, USA

This work has been presented as a poster at the Association for Research in Vision and Ophthalmology (ARVO) Annual Meeting, Baltimore, MD, on May 11th, 2017

Correspondence: David Sarraf, MD, Retinal Disorders and Ophthalmic Genetics Division, Stein Eye Institute, David Geffen School of Medicine at UCLA, Los Angeles, California, +1-310-794-9921, dsarraf@ucla.edu

Funding/Support: The Macula Foundation, Inc., New York, NY, USA

Financial Disclosures: K Bailey Freund is a consultant for Optovue (Fremont, California), Optos (Dunfermline, Scotland), Heidelberg Engineering (Heidelberg, Germany), Genentech (South San Francisco, California) and GrayBug Vision (Redwood City, California); and receives research support from Genentech/Roche (Basel, Switzerland). Pease A Keane is an advisory board member for Heidelberg (Heidelberg, Germany), Allergan (Dublin, Republic of Ireland), Bayer Healthcare (Leverkusen, Germany), Topcon (Tokyo, Japan), Haag-Streit (Köniz, Switzerland) and Novartis (Basel, Switzerland); a consultant for Google DeepMind (London, UK) and Optos; and receives Clinician Scientist award (CS-2014-14-023) from the National Institute for Health Research. The views expressed in this publication are those of the author(s) and not necessarily those of the NHS, the National Institute for Health

Research or the Department of Health. Aaron Nagiel is a consultant for Allergan. Won Ki Lee is a consultant for Bayer Healthcare, Novartis and Santen Pharmaceutical (Osaka, Japan); and receives research support from Allergan. David Sarraf is a consultant for Amgen, Bayer Healthcare, Genentech, Novartis and Optovue; receives research or financial support from Allergan, Genentech, Heidelberg, Optovue, and Regeneron (Tarrytown, New York). The following authors have no financial disclosures: Nopasak Phasukkijwatana, Rosa Dolz-Marco, Mayss Al-Sheikh, Cathy Egan, Sandeep Randhawa, Jay M Stewart, Qingyun Liu, Alex P Hunyor, Allan Krieger, Robert Lalane, Mansour Rahimi, and Lee Merril Jampol.

Key Words and Summary Statement

Key Words: Central serous chorioretinopathy, choroidal folds, choroidal thickness, optic disc edema, pachychoroid disease spectrum

Summary Statement: Peripapillary pachychoroid syndrome is a novel pachychoroid disease spectrum variant in which peripapillary choroidal thickening is associated with intraretinal and/or subretinal fluid. Optic nerve head leakage or edema occurs in some eyes. Peripapillary choroidal congestion exhibiting a compartment syndrome-like effect is proposed as an etiologic mechanism for the peripapillary fluid.

Abstract

Purpose: To describe the features of peripapillary pachychoroid syndrome (PPS), a novel pachychoroid disease spectrum (PDS) entity.

Methods: Medical records of 31 eyes (16 patients) with choroidal thickening associated with intraretinal and/or subretinal fluid in the nasal macula extending from the disc were reviewed (PPS patients). Choroidal thickness was compared to 2 age-matched cohorts: typical PDS (17 eyes with central serous chorioretinopathy or pachychoroid neovasculopathy) and 19 normal eyes.

Results: The PPS patients were 81% male aged 71±7 years. PPS eyes displayed thicker nasal versus temporal macular choroids, unlike PDS eyes with thicker temporal macular choroids ($P<0.0001$). Peripapillary intraretinal and/or subretinal fluid was often overlying dilated Haller layer vessels (pachyvessels). Fundus autofluorescence and fluorescein angiography illustrated peripapillary pigmentary mottling without focal leakage. Most PPS eyes (70%) exhibited other PDS findings including serous pigment epithelial detachment or gravitational tracks. Indocyanine green angiography illustrated dilated peripapillary pachyvessels and choroidal hyperpermeability. The disc was usually crowded, with edema noted in 4/31 (13%) eyes and mild late fluorescein disc leakage identified in half of the cases. Choroidal folds (77%), short axial lengths (39% less than 23 mm) and hyperopia (86%) were common.

Conclusion: PPS is a distinct PDS variant in which peripapillary choroidal thickening is associated with nasal macular intraretinal and/or subretinal fluid and occasional disc edema. Recognition of PPS is important to distinguish it from disorders with overlapping features such as posterior uveitis and neuro-ophthalmologic conditions.

Introduction

The pachychoroid disease spectrum (PDS) refers to a group of retinochoroidal disorders that share distinctive choroidal findings identified with multimodal retinal imaging. These choroidal features include focal or diffuse choroidal thickening associated with reduced fundus tessellation, dilated Haller layer vessels (termed "pachyvessels") with thinning of the overlying inner choroid, and choroidal hyperpermeability demonstrated with indocyanine green angiography (ICGA). The PDS includes pachychoroid pigment epitheliopathy,[1] focal choroidal excavation,[2] central serous chorioretinopathy (CSC),[3] pachychoroid neovasculopathy[4] and polypoidal choroidal vasculopathy.[5]

We have identified a novel PDS variant in which pachychoroid features surround the optic nerve and are associated with intraretinal and/or subretinal fluid and optic nerve head edema in some eyes. Associated findings including serous pigment epithelial detachment (PED), choroidal hyperpermeability, and pachyvessels suggest that this is a pachychoroid-driven entity, rather than a variant of uveal effusion syndrome as was suggested in a single case report.[6] As such, we propose the term peripapillary pachychoroid syndrome (PPS). The aim of this investigation is to report the features of this syndrome and compare this disorder to both normal eyes and two typical PDS entities, CSC and pachychoroid neovasculopathy.

Methods

Subjects

This retrospective, multicenter, observational case series was approved by the University of California Los Angeles Institutional Review Board. The study adhered to the tenets of the Declaration of Helsinki and was conducted in accordance with the Health Insurance Portability and Accountability Act (HIPAA) regulations.

Patients with peripapillary choroidal thickening and intraretinal and/or subretinal fluid in the nasal macular region extending from the temporal margin of the optic disc as noted with optical coherence tomography (OCT) were identified and comprised Group 1. Peripapillary choroidal thickening was defined by the presence of: 1) a thicker choroid than would be expected for age; and/or 2) choroidal thickening associated with Haller vessel dilation and overlying inner choroidal thinning.[1, 3, 4] Patients were excluded from this group if they demonstrated other causes of macular edema, unrelated to a PDS entity, including any evidence of ocular inflammation, macular edema due to diabetic macular edema or retinal vascular occlusion, radiation retinopathy, significant epiretinal membrane formation, any history of intraocular surgery within the last 6 months prior to presentation, or the use of medications known to be associated with cystoid macular edema (CME). Eyes with clinical or imaging evidence of choroidal neovascularization were excluded from this cohort. Patients with cavitary optic disc anomalies (e.g. optic disc pit, optic disc coloboma), optic atrophy, glaucomatous optic neuropathy or ocular tumors were also excluded.

Medical records and multimodal imaging findings were comprehensively reviewed. The data collected included age, sex, past medical history, Snellen visual

acuity (VA), axial length and refraction, and the findings of complete ocular examination. Multimodal imaging included color fundus photography (Carl Zeiss Meditec, Dublin, California, USA; Topcon Medical Systems, Oakland, New Jersey, USA; Optos, Dunfermline, Scotland), spectral domain OCT (SPECTRALIS®, Heidelberg Engineering, Heidelberg, Germany), enhanced depth imaging OCT (EDI-OCT) (SPECTRALIS®, Heidelberg Engineering), swept source OCT (DRI OCT Triton, Topcon Medical Systems), fluorescein angiography (FA) (Carl Zeiss Meditec; SPECTRALIS®, Heidelberg Engineering; Topcon Medical Systems; Optos, Dunfermline, Scotland), indocyanine green angiography (ICGA) (SPECTRALIS®, Heidelberg Engineering) and fundus autofluorescence (FAF) (SPECTRALIS®, Heidelberg Engineering; Optos, Dunfermline, Scotland).

Eleven consecutive patients (17 eyes) greater than or equal to 50 years of age with typical findings of central serous chorioretinopathy (CSC) or pachychoroid neovasculopathy (i.e. patients with typical findings of PDS) were recruited from the practice of DS as a comparative control group and comprised Group 2. CSC was defined by the presence of choroidal thickening within the macula associated with subretinal fluid and corresponding leakage on fluorescein angiography (FA) or macular RPE abnormalities with granular autofluorescence and gravitational tracks. Patients with CSC or pachychoroid features associated with shallow irregular RPE detachment harboring type 1 neovascularization (pachychoroid neovasculopathy) were also included in Group 2. In addition, 19 age-matched normal eyes from 12 patients with no ocular disease other than early cataract or a history of cataract surgery were included as normal control eyes (Group 3).

Image analysis

Choroidal thickness measurement

Choroidal thickness measurements were performed using EDI-OCT images and the caliper tool provided with the review software (Heidelberg Eye Explorer, v1.9.10.0 software, Heidelberg Engineering). Choroidal thickness was defined as the perpendicular distance between Bruch's membrane and the choroidal scleral junction. The measurement was performed on a horizontal section passing through the central fovea at the following positions: (1) the center of the fovea (SF), (2) 1,500 μm nasal to the foveal center (N1.5), (3) 3,000 μm nasal to the foveal center (N3.0), (4) 1,500 μm temporal to the foveal center (T1.5), (5) 3,000 μm temporal to the foveal center (T3.0) and (6) 250 μm temporal to Bruch's membrane origin at the temporal disc margin (BMO250) (Figure 1A). Images were set to an aspect ratio of 1:1 um before each measurement. The hyporeflective band corresponding to the suprachoroidal space when present was not included in the choroidal thickness measurement.[7] If the choroidal scleral junction was not clearly identified, brightness and contrast of the image was adjusted, using the built-in adjustment tool, to best visualize this junction and the outer choroidal border was identified by the line connecting the outer margin of the large choroidal vessel layer. When available, adjacent EDI-OCT scans were reviewed to confirm the accuracy of identifying the choroidal scleral junction. In one patient, choroidal thicknesss was measured on swept source OCT images using Image J 1.51a software[8] with appropriate scales.

Two independent trained graders (NP and MA) performed all the measurements. Large disagreements (>100 μm) over readings were resolved by open adjudication between the readers (2 instances). Measurements from the main reader (NP) were

used for the analysis while those from the second reader (MA) were only used to calculate inter-grader agreement.

Juxtapapillary retinal structures

For Group 1, retinal structures at the temporal disc margin included in the macula OCT scans were evaluated for the presence of intraretinal fluid, subretinal fluid and atrophy of RPE, ellipsoid zone and external limiting membrane (ELM) with associated choroidal signal hypertransmission.

Statistical analysis

Mean choroidal thickness at each position, mean age and visual acuity among the 3 groups were compared. Snellen VA was converted to logarithm of the minimum angle of resolution (LogMAR) for statistical analysis. Ratios of nasal to temporal choroidal thickness were calculated and compared. The differences were tested using Welch's test for analysis of variance with Games-Howell post hoc test for multiple comparisons. Chi-square or Fischer's exact test was used to test differences between proportions. P-value of 0.05 was set as a threshold of significance. Intra-class correlation coefficients (ICC) with 95% confidence intervals (CIs) were calculated to evaluate inter-grader agreement. Statistical analysis was performed using PASW Statistics for Windows, Version 18.0 (SPSS, Inc, Chicago, Illinois, USA)

Results

A total of 31 eyes from 16 patients with peripapillary choroidal thickening associated with intraretinal and/or subretinal fluid extending from the temporal disc margin into the macula were identified (Group 1) comprising 13 males and 3 females with a mean age of 71 years (standard deviation [SD] 7 years, range 58-86 years).

In Group 1, the choroid was thickened preferentially in the nasal macular region in contradistinction to those eyes with typical PDS and normal eyes as illustrated in Figure 1. Axial length (18 eyes) or manifest refraction (14 eyes) was available in 20 eyes and nearly all (12 of 14 eyes) were hyperopic with a mean (±SD) spherical equivalence of + 2.5 (±2.2) diopters. Axial lengths ranged from 20.00 mm to 24.59 mm (7 of 18 eyes (39%) had axial lengths less than 23 mm) with a mean±SD of 22.9±1.3 mm. Choroidal folds were present in 24 of 31 (77%) eyes often along the vascular arcades (Figures 4-6). The optic disc cup was small in most eyes with 18 of 31 (58%) eyes with a cup less than 0.3 and 10 of 31 (32%) with cupping of 0.1 or with a crowded disc (Figures 4 and 6). Chronic bilateral disc edema (Figure 7) was identified in 2 patients with normal neurological evaluations that included unremarkable magnetic resonance imaging (MRI) of the brain and orbit and normal lumbar puncture. VA in our PPS patients was relatively good. The majority of patients (65%, 20/31 eyes) demonstrated a VA of 20/30 or better. Anatomical features associated with reduced VA were intraretinal cysts approaching the foveal center, subfoveal fluid, and ellipsoid zone or RPE attenuation at the center of the fovea. The presence of optic disc edema without the above anatomical foveal abnormalities did not correlate with reduced VA. Demographic and clinical data are summarized in Table 1.

Of the 31 Group 1 eyes, FA was available in 29 eyes and FAF was available in 25 eyes. Peripapillary RPE alterations were identified in all 29 eyes with corresponding mottled autofluorescence or granular transmission hyperfluorescence on FA without focal areas of leakage. On FA, all eyes demonstrated late hyperfluorescent staining in a ring-like configuration surrounding the optic disc with mild diffuse leakage in 14 eyes (Figure 8) and questionable mild leakage in another 10 eyes. Hyperautofluorescent patches in the posterior pole were found in 10 of 25 eyes with FAF assessment (Figures 2, 4, 6). Gravitational tracks of pigmentary abnormalities on either FA or FAF were illustrated in 8 of 31 eyes (Figures 2, 6). ICGA was available in 11 eyes and illustrated peripapillary dilated choroidal vessels with multifocal hyperpermeability in 9 eyes (Figures 2, 6).

In addition to choroidal hyperpermeability, most eyes (19/27, 70%) exhibited other features of the PDS including serous PED (13/31, 42%), FAF evidence of prior serous retinal detachment outside the peripapillary region (15/25, 60%) and a gravitational track of RPE alteration (8/31, 26%) (Figure 2, 6).

Retinal structures at disc margins were studied by OCT. All eyes illustrated intraretinal fluid and cysts extending from the temporal disc margin with associated atropy of the RPE, ellipsoid zone and external limiting membrane (Figures 2-7). These atrophic areas of the RPE and outer retina resulted in choroidal signal hypertransmission at the optic disc margin in all eyes. Varying amounts of subretinal fluid were present in 23 of 31 eyes. OCT B-scans over the optic discs were available in 18 eyes, 11 of which demonstrated intraretinal fluid at the nasal disc margin (Figures 2 and 7).

To more accurately assess the significance of the choroidal thickness of the 31 eyes in Group 1, comparative control groups were recruited to the study. Group 2 was comprised of 17 eyes from 11 patients and included eyes with typical CSC (13 eyes from 8 patients) or eyes with pachychoroid neovasculopathy (4 eyes from 3 patients). Group 3 was comprised of 19 normal eyes from 12 age-matched controls. The mean age was not statistically different between the 3 groups (P=0.117) but there were more females in Group 3 (Table 2). There was an excellent agreement in choroidal thickness measurements between the two readers with an intra-class correlation coefficient (ICC) of 0.996 (95% CI, 0.995-0.997).

Analysis of choroidal thickness demonstrated significant differences among the three groups (Figure 9). The mean choroidal thickness in Group 1 (PPS) and Group 2 (typical PDS) was significantly greater than Group 3 (normal) at all 6 measured positions ($p<0.01$) except for position T3.0 where the difference between Group 1 and Group 3 was not statistically different ($p=0.06$). Interestingly, Groups 1 and 2 illustrated different choroidal thickness profiles. Mean subfoveal choroidal thickness was not statistically different between these 2 groups; however, the mean choroidal thickness in the nasal macula in Group 1 was significantly greater than that of Group 2 at positions N1.5 and N3.0 (P=0.038 and 0.006, respectively). The choroidal thickness of Group 1 then decreased sharply from the center position towards the temporal macula and was thinner than Group 2 temporally. In Group 1, the temporal macular choroid was even thinner than the nasal side. In contrast, the temporal macular choroid of Group 2 remained relatively thicker than the nasal side, demonstrating the same pattern as Group 3 (normal).

As the choroidal thickness was evidently thickened in the peripapillary region in Group 1, we performed an additional analysis of the ratio of nasal to temporal choroidal thickness. The ratios of choroidal thickness at N3.0 to T3.0 were 1.33±0.60, 0.64±0.18 and 0.49±0.17 for Groups 1, 2 and 3, respectively. The ratios of choroidal thickness at BMO250 to T3.0 were 0.65±0.23, 0.35±0.13 and 0.31±0.14 for Groups 1, 2 and 3, respectively. Furthermore, the ratios of the sum of choroidal thickness at N1.5 and N3.0 to the sum of that at T1.5 and T3.0 were 1.36±0.43, 0.80±0.18 and 0.65±0.20 for Groups 1, 2 and 3, respectively. The differences between all these ratios of Group 1 versus Group 2 were all statistically significant ($P<0.00001$). Figure 10 demonstrates the distribution of eyes with various ratios of nasal to temporal choroidal thickness. Group 1 was considerably different from Groups 2 and 3. There were no eyes with an N3.0/T3.0 ratio greater than 1 in Groups 2 and 3 while 23/31 (74%) of eyes in Group 1 had an N3.0/T3.0 ratio greater than 1 ($P<10^{-8}$).

Data regarding treatment response were available for some study eyes. Three eyes treated with intravitreal anti-vascular endothelial growth factor therapy illustrated no response. One eye had resolution of macular fluid following verteporfin photodynamic therapy, while 2 other eyes showed no response. Two eyes treated with topical dorzolamide had resolution of macular fluid, while 1 eye showed minimal improvement. Oral acetazolamide in one patient was not associated with a reduction in macular fluid. One eye had spontaneous resolution of fluid with observation.

Discussion

We studied eyes with peripapillary choroidal thickening associated with intraretinal and/or subretinal fluid extending from the temporal disc margin into the macula. Our analysis demonstrated that the nasal macular choroid was significantly thicker than the temporal macular choroid in these eyes (Group 1), especially when compared to normal or typical PDS eyes. Most PPS eyes demonstrated choroidal folds (24/31, 77%), a relatively short axial length (7 of 18 eyes (39%) with axial lengths less than 23 mm) and a hyperopic refractive error (12/14, 86%). Many eyes (11/18, 61%) with available OCT B-scans through the optic disc also illustrated intraretinal fluid on the nasal side of the nerve. The optic disc of these patients were typically crowded and a small cup was identified in more than half of the cases with optic disc edema noted in 4 eyes of 2 cases. This unique clinical presentation prompted us to coin the term peripapillary pachychoroid syndrome (PPS). The findings of PPS were bilateral in 15 of our 16 cases.

Our analysis illustrated that the pattern of choroidal thickness in our PPS eyes was significantly ($P < 0.0001$) different than that of typical PDS entities such as CSC and pachychroid neovasculopathy and normal controls. Studies have illustrated that the macular choroidal thickness is normally greatest in the subfoveal position followed by the temporal and nasal positions, respectively.[9, 10] This was remarkably different from the pattern identified in PPS eyes in which the nasal macular choroid was disproportionately thicker with associated pachyvessels compared to normal or typical PDS eyes and often thicker than the temporal macular choroid of the same eye (Figures 1, 9 and 10). Peripapillary choroidal thickening was associated with

peripapillary RPE mottling on FAF or FA in all cases, but FA did not show focal leakage. Mild optic disc leakage was observed in 14/29 (48%) eyes without evidence of ocular inflammation (Figure 8). ICGA demonstrated dilated peripapillary large choroidal vessels with multifocal choroidal hyperpermeability identified in the mid-phase ICGA.

The association of PPS with choroidal folds, short axial length and hyperopia indicated similarities with uveal effusion syndrome (UES), although there was no evidence of serous choroidal detachment in any of our cases. Recent case reports,[6, 11] with very similar findings to our cases of PPS, have applied the term 'isolated posterior uveal effusion' to describe a syndrome characterized by a thick posterior choroid with serous macular detachment, nasal cystoid macular edema, choroidal folds and short axial length without peripheral retinochoroidal detachment. However, we believe that our cases illustrated more in common with PDS rather than a form of UES for the following reasons: 1) Our patients often displayed serous RPE detachment and gravitational tracks of RPE alteration, which are commonly seen in PDS and have not been described in UES. In addition, pigmentary changes in a leopard-spot patterns characteristic of UES were not identified in our patients; 2) ICGA in our patients was very characteristic for PDS, including dilated large choroidal veins (pachyvessels) and choroidal hyperpermeability.[1, 4, 12, 13] The pachyvessels were identified during dye transit and washed out in the late phase of the study. These pachyvessels correspond to dilated Haller layer vessels visible on structural EDI-OCT, which typically show attenuation of overlying Sattler layer and choriocapillaris. ICGA hyperpermeability was typically focal or multifocal, best seen during the mid-phase of the study, and often was observed around the washed out silhouettes of the

pachyvessels. This hyperpermeability often faded in the late phase of the ICGA. In contrast, Uyama et al, 2000[14] reported the ICGA pattern in UES as a diffusely granular hyperfluorescence in the very early phase, which increased with time and persisted until the late phase of the study as a diffuse intense choroidal hyperfluorescence; 3) The location of abnormal findings predominantly around the optic nerve and in the nasal macula was not consistent with UES and was much more typical of PDS/CSC. Hence, we prefer the term "peripapillary pachychoroid syndrome" for this entity. We have refined the clinical picture demonstrating that, unlike most other PDS disorders, the choroid in PPS is preferentially thickened in the nasal macula compared to the temporal macula. It is believed that the primary abnormality of the pachychoroid spectrum disorders relates to dilated choroidal vessels[3-5] whereas in UES, a reduced fluid and protein permeability of the sclera is the main mechanism.[14, 15] It is possible that reduced scleral permeability with older age[16, 17] may exacerbate peripapillary choroidal congestion in patients with PPS, giving rise to some overlapping findings with UES.

A recent large case series of eyes with chorioretinal folds caused by various ocular disorders identified eyes with mottled hyperfluorescence in the peripapillary and/or macular regions similar to our cases.[18] However, EDI-OCT and choroidal imaging was not performed in these eyes. According to the findings of our study, PPS should also be considered in the differential diagnosis of chorioretinal folds.

While certain findings in PPS eyes were suggestive of chronic CSC, another PDS entity, there were important distinguishing features. Overlapping findings included serous PED, gravitational tracks, evidence of serous retinal detachment outside the peripapillary region with FAF, and outer retinal atrophy in the majority (19/27, 70%) of

PPS eyes (Figures 2, 6). Also, a male preponderance (13/16, 81%) and the ICGA findings of pachyvessels and hyperpermeability were similar to that of CSC. The most important feature distinguishing PPS from CSC was the preferential choroidal thickening in the peripapillary region as demonstrated in Figures 1, 9 and 10. The choroidal thickness profile was significantly different from typical CSC in that the nasal choroid was thickened and the thickness sharply decreased towards the temporal side. Other useful distinguishing features included the presence of choroidal folds, older age and a small cup to disc ratio with mild disc leakage with late FA, not commonly present in CSC.

Multimodal imaging analysis in our study suggested that the primary abnormality of PPS resided in the peripapillary choroid where the characteristic PDS findings of ICGA hyperpermeability and pachyvessels were observed. Peripapilllary choroidal congestion in PPS may lead to high hydrostatic pressure under the RPE causing RPE dysfunction and leakage of fluid into the subretinal space as has been postulated in the context of CSC.[14, 19] This hydrostatic pressure may be subject to a compartment-like syndrome (if choroidal outflow is disrupted) and may compress the optic nerve leading to complications including crowded disc, optic disc edema and/or optic disc leakage. Growing evidence of peripapillary pachychoroid exerting pressure stress on the optic nerve has recently emerged as a contributing factor for acquired lamina cribosa defects[20] and nonarteritic anterior ischemic optic neuropathy (NAION).[21] The reason why the choroid is congested preferentially in the peripapillary region is unclear. Interestingly, choroidal venous drainage from the peripapillary choroidal region has been studied histologically.[22] These veins penetrate the sclera around the optic nerve and enter the pia mater of the nerve and are called choroidopial veins. Whether there

is an increased resistance of choroidal venous outflow through these choroidopial veins or the vortex veins in PPS requires further investigations.

The mechanism of intraretinal fluid extension from the disc margin in PPS is unclear. Fluorescein leakage was minimal in PPS eyes and angiographic CME was not appreciated in these cases. It has been suggested that intraretinal cystic fluid may originate from the congested choroid through regions of peripapillary atrophy (PPA) and associated atrophy of the RPE and ELM that normally serve as barriers for fluid to enter the retina.[6] In the present study, atrophy of the RPE and ELM and corresponding choroidal signal hypertransmission at the temporal disc margins were detected by spectral domain OCT in all cases even in cases without frank PPA, and these juxtapapillary atrophic areas may facilitate fluid entry into the retina. Whether these atrophic areas are secondary to chronic hydrostatic stress to the optic disc margin from the congested peripapillary choroid or secondary to the presence of chronic subretinal fluid because of RPE dysfunction requires further longitudinal investigation. Alternatively, the intraretinal cysts without FA leakage may represent degenerative cavitation as has been described in the context of chronic CSC[23-25] although the presence of SRF and large exudative-like retinal cysts in many cases makes cavitation unlikely.

A recent study by Lee et al., described the presence of lamina cribosa defects or disinsertions as a potential source of intraretinal fluid extending from the disc without leakage on FA in patients with pachychoroid disorders and patients with glaucomatous optic neuropathy.[20] This study has proposed that a thickened choroid could stress the optic nerve head margin and lead to a lamina cribosa defect or disinsertion and subsequent intraretinal fluid. Our study was retrospective and did not employ an EDI-

OCT raster protocol with sufficient density to detect such defects. Of note, the pachychoroid subjects in Lee's study appeared to be different from ours as Lee's study excluded eyes with peripapillary intraretinal fluid associated with RPE atrophy (peripapillary fluid and RPE atrophy were found in all cases in our study) and only 2 of 8 eyes illustrated late staining of the optic nerve border (as opposed to all eyes in our study). Also, it was not clear in their study if the macular choroid was preferentially thickened nasally as in PPS. Furthermore, the lamina cribosa defects were not detected in about half of their pachychoroid patients. This indicates that there may be more than one mechanism of intraretinal fluid accumulation.

The association of a crowded disc appearance or optic disc edema with PPS is interesting. Sarraf and Schwartz[26], before the OCT era, described 3 cases of bilateral choroidal folds and short axial length associated with crowded disc and FA leakage in one eye and optic atrophy in the fellow eye. They excluded neurological disorders including idiopathic intracranial hypertension and proposed that idiopathic acquired hyperopia and shrinkage of the scleral canal could lead to a crowded disc syndrome and the development of NAION. Some of our cases shared similar features of small optic cups, optic disc leakage, short axial lengths and choroidal folds. These findings were similar to the crowded disc syndrome cases described by Sarraf and Schwartz[26] and it is possible that these cases would have demonstrated PPS with current multimodal imaging capabilities. As mentioned above, a finding of peripapillary pachychoroid has recently been implicated in NAION.[21] Whether PPS patients have a higher incidence of NAION requires further investigations, however.

It should be acknowledged that some eyes in our study could be classified with more than one PDS disorder (hence the term "spectrum"). PPS is best defined by the

presence of characteristic peripapillary abnormalities. In some eyes, this may be the primary pathology, but in others, these findings may be more of an incidental finding detected during an evaluation of some other disorders of the PDS such as CSC or polypoidal choroidal vasculopathy. In this study, eyes with type 1 neovascularization were excluded from Group 1 analysis. However, PPS may be associated with type 1 neovascularization with or without polyps.

Limitations of this analysis included the retrospective nature of the study, incomplete data collection and incomplete multimodal imaging in some cases, and the relatively small sample size. Choroidal analysis was compared with control eyes using a single-line EDI-OCT scan through the foveal center. Future prospective and longitudinal studies with comparative volumetric OCT scans would be valuable to corroborate our findings.

In summary, we have described a new subgroup in the PDS referred to as peripapillary pachychoroid syndrome (PPS) and characterized by a relatively thickened nasal macular choroid (versus the temporal choroid) with associated intraretinal and subretinal fluid in the nasal macular region extending from the disc margin. Intraretinal and subretinal fluid can also be identified nasal to the optic disc. Focal RPE and ELM atrophy at the disc margin and corresponding choroidal hypertransmission were identified in all eyes and may indicate the site of fluid entry into the retina. FAF and FA illustrated peripapillary mottling of the RPE with late staining, but minimal or no leakage. ICGA demonstrated pachyvessels and multifocal hyperpermeability in the peripapillary region. The optic nerve head was usually crowded and occasionally edematous with mild late leakage with FA. Patients with PPS were mostly male, but typically older than those with CSC. Choroidal folds, a relatively short axial length and

hyperopia were common associations. Peripapillary choroidal congestion with a compartment-like effect on the peripapillary region was proposed as an etiologic mechanism. While PPS may be considered in the spectrum of pachychoroid disorders such as CSC, the aggregate of presenting features are sufficiently characteristic as to be considered a unique syndrome. It is important to recognize PPS and distinguish this new clinical entity from similar disorders such as posterior uveitis and neuro-ophthalmologic conditions that can share overlapping features, namely disc leakage and edema.

References

1. Warrow DJ, Hoang QV, Freund KB. Pachychoroid pigment epitheliopathy. Retina 2013; 33:1659-1672.

2. Chung H, Byeon SH, Freund KB. Focal choroidal excavation and its association with pachychoroid spectrum disorders: A Review of the Literature and Multimodal Imaging Findings. Retina 2017; 37:199-221.

3. Dansingani KK, Balaratnasingam C, Naysan J, Freund KB. En Face Imaging of Pachychoroid Spectrum Disorders with Swept-Source Optical Coherence Tomography. Retina 2016; 36:499-516.

4. Pang CE, Freund KB. Pachychoroid neovasculopathy. Retina 2015; 35:1-9.

5. Balaratnasingam C, Lee WK, Koizumi H et al. Polypoidal Choroidal Vasculopathy: A Distinct Disease or Manifestation of Many? Retina 2016; 36:1-8.

6. Pautler SE, Browning DJ. Isolated posterior uveal effusion: expanding the spectrum of the uveal effusion syndrome. Clin Ophthalmol 2015; 9:43-49.

7. Yiu G, Pecen P, Sarin N et al. Characterization of the choroid-scleral junction and suprachoroidal layer in healthy individuals on enhanced-depth imaging optical coherence tomography. JAMA Ophthalmol 2014; 132:174-181.

8. Schneider CA, Rasband WS, Eliceiri KW. NIH Image to ImageJ: 25 years of image analysis. Nat Methods 2012; 9:671-675.

9. Shin JW, Shin YU, Lee BR. Choroidal thickness and volume mapping by a six radial scan protocol on spectral-domain optical coherence tomography. Ophthalmology 2012; 119:1017-1023.

10. Margolis R, Spaide RF. A pilot study of enhanced depth imaging optical coherence tomography of the choroid in normal eyes. Am J Ophthalmol 2009; 147:811-815.

11. Liu Q, Hemarat K, Kayser DL, Stewart JM. A Case of Posterior Uveal Effusion Syndrome Masquerading as Uveitis. Retin Cases Brief Rep 2016; 11 Suppl 1:S124-S127.

12. Dansingani KK, Balaratnasingam C, Klufas MA et al. Optical Coherence Tomography Angiography of Shallow Irregular Pigment Epithelial Detachments In Pachychoroid Spectrum Disease. Am J Ophthalmol 2015; 160:1243-1254 e1242.

13. Ersoz MG, Arf S, Hocaoglu M et al. Indocyanine Green Angiography of Pachychoroid Pigment Epitheliopathy. Retina 2017.

14. Uyama M, Takahashi K, Kozaki J et al. Uveal effusion syndrome: clinical features, surgical treatment, histologic examination of the sclera, and pathophysiology. Ophthalmology 2000; 107:441-449.

15. Elagouz M, Stanescu-Segall D, Jackson TL. Uveal effusion syndrome. Surv Ophthalmol 2010; 55:134-145.

16. Jackson TL, Hussain A, Morley AM et al. Scleral hydraulic conductivity and macromolecular diffusion in patients with uveal effusion syndrome. Invest Ophthalmol Vis Sci 2008; 49:5033-5040.

17. Stewart JM, Schultz DS, Lee OT, Trinidad ML. Exogenous collagen cross-linking reduces scleral permeability: modeling the effects of age-related cross-link accumulation. Invest Ophthalmol Vis Sci 2009; 50:352-357.

18. Olsen TW, Palejwala NV, Lee LB et al. Chorioretinal folds: associated disorders and a related maculopathy. Am J Ophthalmol 2014; 157:1038-1047.

19. Guyer DR, Yannuzzi LA, Slakter JS et al. Digital indocyanine green videoangiography of central serous chorioretinopathy. Arch Ophthalmol 1994; 112:1057-1062.

20. Lee JH, Park HY, Baek J, Lee WK. Alterations of the Lamina Cribrosa Are Associated with Peripapillary Retinoschisis in Glaucoma and Pachychoroid Spectrum Disease. Ophthalmology 2016; 123:2066-2076.

21. Nagia L, Huisingh C, Johnstone J et al. Peripapillary Pachychoroid in Nonarteritic Anterior Ischemic Optic Neuropathy. Invest Ophthalmol Vis Sci 2016; 57:4679-4685.

22. Ruskell GL. Peripapillary venous drainage from the choroid: a variable feature in human eyes. Br J Ophthalmol 1997; 81:76-79.

23. Iida T, Yannuzzi LA, Spaide RF et al. Cystoid macular degeneration in chronic central serous chorioretinopathy. Retina 2003; 23:1-7; quiz 137-138.

24. Piccolino FC, De La Longrais RR, Manea M, Cicinelli S. Posterior cystoid retinal degeneration in central serous chorioretinopathy. Retina 2008; 28:1008-1012.

25. Piccolino FC, De La Longrais RR, Manea M et al. Risk factors for posterior cystoid retinal degeneration in central serous chorioretinopathy. Retina 2008; 28:1146-1150.

26. Sarraf D, Schwartz SD. Bilateral choroidal folds and optic neuropathy: a variant of the crowded disk syndrome? Ophthalmology 2003; 110:1047-1052.

Figure legends.

Figure 1. Enhanced depth imaging optical coherence tomography of the macula and choroid. A, Positions of choroidal thickness measurement used in this study. BMO250, 250 μm temporal to Bruch's membrane origin at the temporal disc margin; N1.5, 1,500 μm nasal to the foveal center; N3.0, 3,000 μm nasal to the foveal center; SF, subfoveal ;T1.5, 1,500 μm temporal to the foveal center; T3.0, 3,000 μm temporal to the foveal center. B, Normal left eye of a 71-year-old female. C, Left eye of a 69-year-old male with typical chronic central serous chorioretinopathy. D, Left eye of a 75-year-old male with peripapillary pachychoroid syndrome. Note the peripapillary intraretinal cysts (arrow) and disproportionate thickening of the nasal choroid associated with choroidal folds in D versus the tapering nasal choroid in B and C. Further, there are more dilated large choroidal vessels (pachyvessels) on the nasal side compared to the temporal side in D. White asterisks denote pachyvessels with associated thinning of the overlying inner choroid. Choroidal thickness is outlined with arrowheads.

Figure 2. Multimodal imaging of a 63-year-old male with peripapillary pachychoroid syndrome. A and B, Fundus autofluorescence illustrates hypoautofluorescent peripapillary atrophy (PPA) and large areas of peripapillary mottled autofluorescence in both eyes. Hyperautofluorescent patches are illustrated superotemporal in the left eye and inferior in both eyes and correspond to outer retinal atrophy similar to chronic central serous chorioretinopathy. C and D, Late phase fluorescein angiography illustrates speckled hyperfluorescent window defects and staining surrounding the optic disc and intense staining of PPA in both eyes. There is no distinct leakage. E and F,

Early phase indocyanine green angiography (ICGA) illustrates peripapillary dilated large choroidal vessels (pachyvessels) (arrows). G and H, Mid to late phase ICGA illustrates multifocal peripapillary choroidal hyperpermeability. I and J, Optical coherence tomography (OCT) through the optic discs of the right (G) and left (H) eyes illustrates intraretinal fluid in both the nasal and temporal regions of the optic discs with associated choroidal hypertransmission (arrows) and atrophy of the retinal pigment epithelium, ellipsoid zone and external limiting membrane. Note the peripapillary pachyvessels (asterisks). K and L, Swept-source OCT illustrates intraretinal fluid in the nasal macula and a thickened choroid (outlined by arrowheads) with pachyvessels (asterisks) more prominent in the nasal versus the temporal areas. Note the presence of subretinal fluid in both eyes.

Figure 3. Multimodal imaging of an 82-year-old male with peripapillary pachychoroid syndrome. A and B, Fundus autofluorescence illustrates mottled autofluorescence of the retinal pigment epithelium (RPE) in the peripapillary region. C and D, Late phase fluorescein angiography illustrates peripapillary RPE window defects and mottled fluorescence without focal leakage in each eye. Note the peripapillary hyperfluorescent rings with mild late leakage in both eyes. E and F, Early phase indocyanine green angiography (ICGA) illustrates dilated large choroidal vessels or pachyvessels (arrows) predominantly in the nasal macula and peripapillary region in both eyes. G and H. Mid to late phase ICGA illustrates multifocal choroidal hyperpermeability in areas corresponding to the pachyvessels. I and J, Enhanced depth imaging optical coherence tomography illustrates intraretinal fluid with cysts in the nasal macula extending from the temporal optic disc margin and associated with focal RPE, ellipsoid

zone and external limiting membrane atrophy (solid arrows) in both eyes. Note the presence of RPE atrophy and the corresponding choroidal signal hypertransmission (dash arrows) in the peripapillary area in each eye. Note the thickened nasal macular choroid (outlined by arrowheads) associated with pachyvessels (asterisks) and thinning of the overlying inner choroid. The pachyvessels are more prominent in the nasal than temporal sides of the macula, similarly identified by ICGA.

Figure 4. A 70-year-old man with peripapillary pachychoroid syndrome. A and B, Fundus autofluorescence illustrates hypoautofluorescent peripapillary atrophy and mottled autofluorescence at the temporal disc margin in both eyes with adjacent hyperautofluorescent patches. C and D, Optical coherence tomography (OCT) through the optic nerve of the right (C) and left (D) eyes illustrates intraretinal fluid extending from the temporal disc margin. E and F, Enhanced depth imaging OCT illustrates intraretinal cysts in the nasal macula extending from the disc margin with associated peripapillary atrophy with ellipsoid zone and external limiting membrane atrophy (solid arrows). Note the corresponding choroidal signal hypertransmission adjacent to the disc margins (dash arrows). The choroid is thicker with more dilated large choroidal vessels (asterisks) on the nasal side compared to the temporal side (outlined by arrowheads). G and H, OCT scans of the right (G) and left (H) eyes at the level of the green lines in A and B, respectively, illustrate choroidal folds.

Figure 5. Multimodal imaging of a 69-year-old male with peripapillary pachychoroid syndrome. A and B, Fundus autofluorescence illustrates the predominant distribution of retinal pigment epithelium (RPE) abnormalities in the peripapillary region of both eyes.

Alternate hyperautofluorescent and hypoautofluorescent bands of the choroidal folds are illustrated in the left eye (arrows). C and D, Enhanced depth imaging optical coherence tomography illustrates intraretinal cysts in the nasal macula that extend from the optic disc margin with associated atrophy of the RPE, ellipsoid zone, external limiting membrane and corresponding choroidal signal hypertransmission (arrows). Note also the presence of small pigment epithelial detachments in both eyes and subretinal fluid in the left eye. The choroid is thickened with more dilated large choroidal vessels predominantly in the nasal and central regions compared to the temporal area in each eye (outlined by arrowheads).

Figure 6. Multimodal imaging of a 69-year-old male with peripapillary pachychoroid syndrome. A and B, Color fundus photographs illustrate juxtapapillary hard exudates in both eyes, mild pigmentary changes inferior to disc in the right eye and a chorioretinal scar temporal to the macula in the left eye. Note the presence of choroidal folds (arrowheads) in the right eye and a small cup to disc ratio in both eyes. C and D, Fundus autofluorescence illustrates mild mottled autofluorescence temporal to the right disc and inferior to the left disc. A hyperautofluorescent patch superior to the disc and mottled autofluorescence inferior to the disc in a gravitational pattern are illustrated in the right eye. There are hyperautofluorescent patches inferonasal to the disc, superior to the fovea and concentric to the hypoautofluorescent scar in the left eye. E and F, Fluorescein angiography illustrates multiple foci of window defects with late staining in the macula and peripapillary region, and multiple small pigment epithelial detachments in the right eye with a speckled hyperfluorescent gravitational tract extending from the disc inferiorly in the right eye. A hypofluorescent scar with late

staining and variable staining in the peripapillary region are noted in the left eye. No significant fluorescein leakage is identified in either eye. Note the alternate hyperfluorescent and hypofluorescent bands of choroidal folds superotemporally in the right eye greater than the left eye (arrowheads). G-J, Indocyanine green angiography (ICGA). Early ICGA (G and I) illustrates dilated large choroidal vessels in the peripapillary region and central macula with corresponding multifocal hyperpermeability in the mid-phase ICGA (H and J) in both eyes. K and L, Enhanced depth imaging optical coherence tomography illustrates intraretinal fluid in the nasal macula extending from the disc margins with associated atrophy of the retinal pigment epithelium, ellipsoid zone, external limiting membrane and corresponding choroidal signal hypertransmission (arrows) in both eyes. A temporal chorioretinal scar with surrounding intraretinal cysts and subfoveal fluid are also illustrated in the left eye. Note the thickened choroid (outlined by arrowheads) and dilated large choroidal vessels predominantly within the nasal region of each eye.

Figure 7. Multimodal imaging of a 71-year-old male with peripapillary pachychoroid syndrome and chronic bilateral optic disc edema for over 1 year. The patient initially presented with bilateral enlarged blind spots and meticulous neurological workup including magnetic resonance imaging of the brain and orbits, lumbar puncture and cerebrospinal fluid analysis and infectious serology were all negative. A and B, Enhanced depth imaging optical coherence tomography (OCT) illustrates intraretinal fluid in the nasal macula extending from the optic disc margin in each eye and subretinal fluid in the left eye. Atrophy of the retinal pigment epithelium (RPE), ellipsoid zone, and external limiting membrane is noted at the temporal disc margins and

associated with corresponding choroidal signal hypertransmission (arrows). The choroid is thick with dilated large choroidal vessels more prominent in the nasal versus the temporal side in both eyes (outlined by arrowheads). C and D, OCT through the optic nerve head illustrates the presence of disc edema and intraretinal cysts surrounding the optic disc.

Figure 8. Late fluorescein angiography illustrates peripapillary hyperfluorescent rings with mild late leakage in right and left eyes of 4 cases with peripapillary pachychoroid syndrome.

Figure 9. This graph illustrates choroidal thickness at different positions in the macula of eyes with peripapillary pachychoroid syndrome (PPS). A distinctive choroidal thickness profile is noted. The nasal choroid is significantly thicker and sharply thins out toward the temporal side in the group of eyes with PPS versus the normal and the typical pachychoroid disease spectrum (PDS) groups. Group 1, PPS; Group 2, typical PDS (central serous chorioretinopathy or pachychoroid neovasculopathy); Group 3, age-matched normal eyes; BMO250, 250 μm temporal to Bruch's membrane origin; N3.0, 3,000 μm nasal to the foveal center; N1.5, 1,500 μm nasal to the foveal center; SF, subfoveal; T1.5, 1,500 μm temporal to the foveal center; T3.0, 3,000 μm temporal to the foveal center. P-values were significant when the designated intervals were compared and * denotes $P<0.05$ and ** denotes $P<0.01$.

Figure 10. Histograms illustrating distributions of different ratios of nasal to temporal choroidal thickness in each group. A, Ratio of choroidal thickness: BMO250 over T3.0.

B, Ratio of choroidal thickness: N3.0 over T3.0. C, Ratio of nasal to temporal choroidal thickness [N/T = (N1.5+N3.0)/(T1.5 + T3.0)]. The distribution of nasal to temporal choroidal thickness ratios illustrate a shift towards a value of 1 or greater for Group 1 (unlike Groups 2 and 3) indicating that the nasal choroid is thicker than the temporal choroid in contrast to Groups 2 and 3. P-values indicate comparisons of the mean ratios between each group. The differences between Group 1 vs Group 2 and Group 1 vs Group 3 were highly statistically significant. Group 1,peripapillary pachychoroid syndrome; Group 2, typical pachychoroid disease spectrum (central serous chorioretinopathy or pachychoroid neovasculopathy); Group 3, age-matched normal eyes; BMO250, 250 μm temporal to Bruch's membrane origin; N3.0, 3,000 μm nasal to the foveal center; N1.5, 1,500 μm nasal to the foveal center; T1.5, 1,500 μm temporal to the foveal center; T3.0, 3,000 μm temporal to the foveal center

Fig 1

Click here to download Figure (Please type in the figure number in the Description Box; Fig 1, Fig 2, etc.) Figure 1.tiff

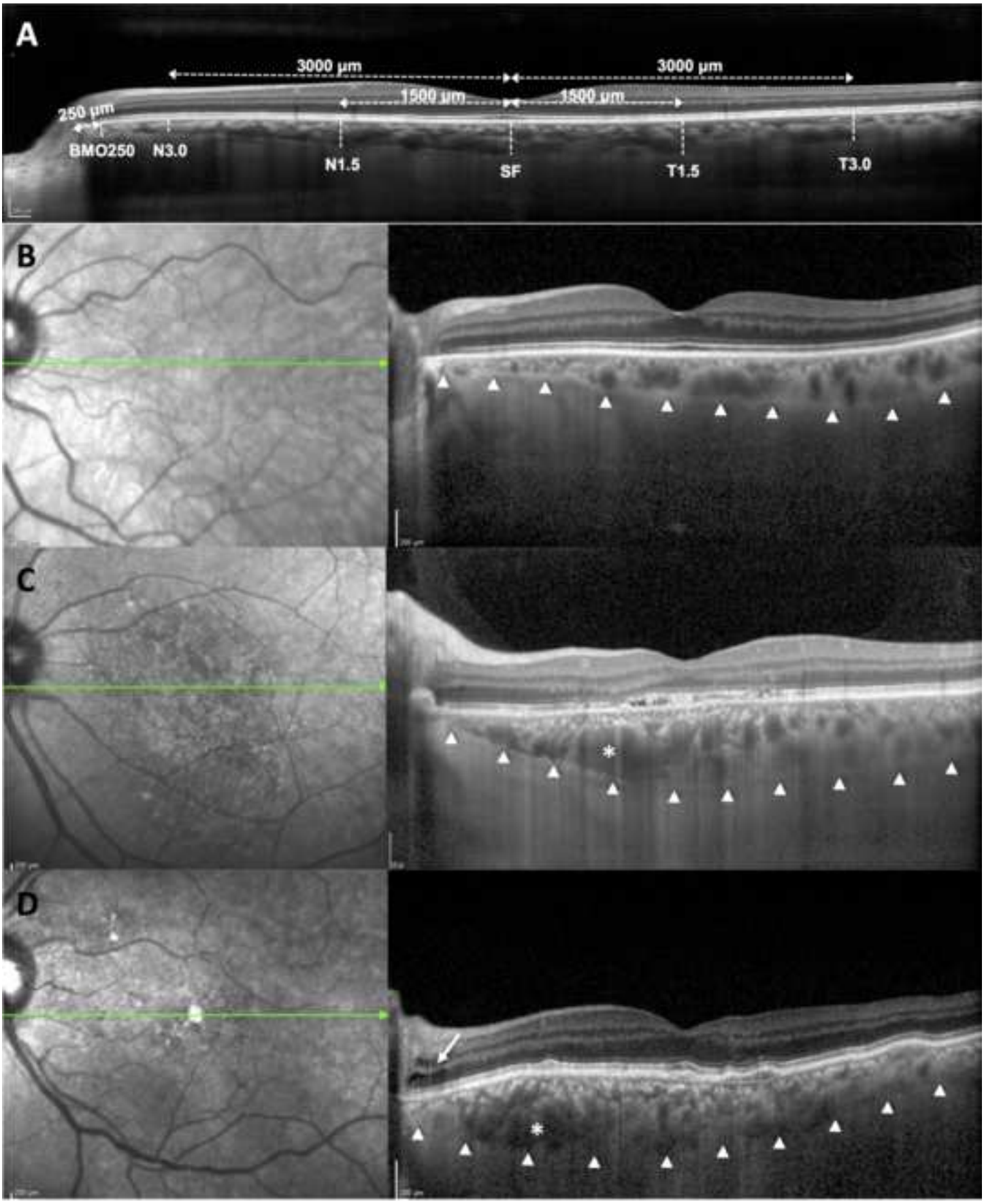

Fig 2

Click here to download Figure (Please type in the figure number in the Description Box; Fig 1, Fig 2, etc.) Figure 2.tiff

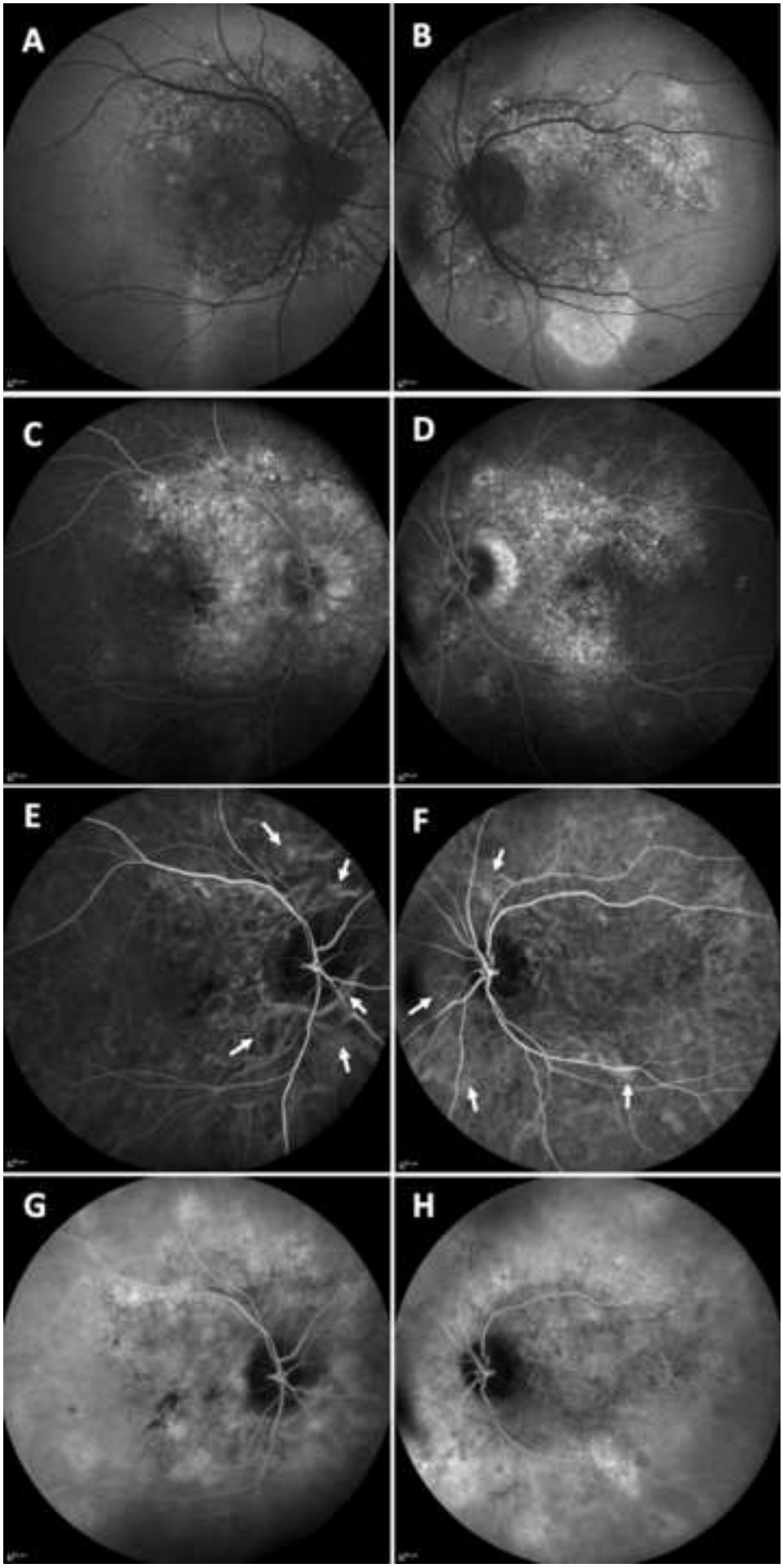

Fig 2 continued

Click here to download Figure (Please type in the figure number in the Description Box; Fig 1, Fig 2, etc.) Figure 2 cont.tiff

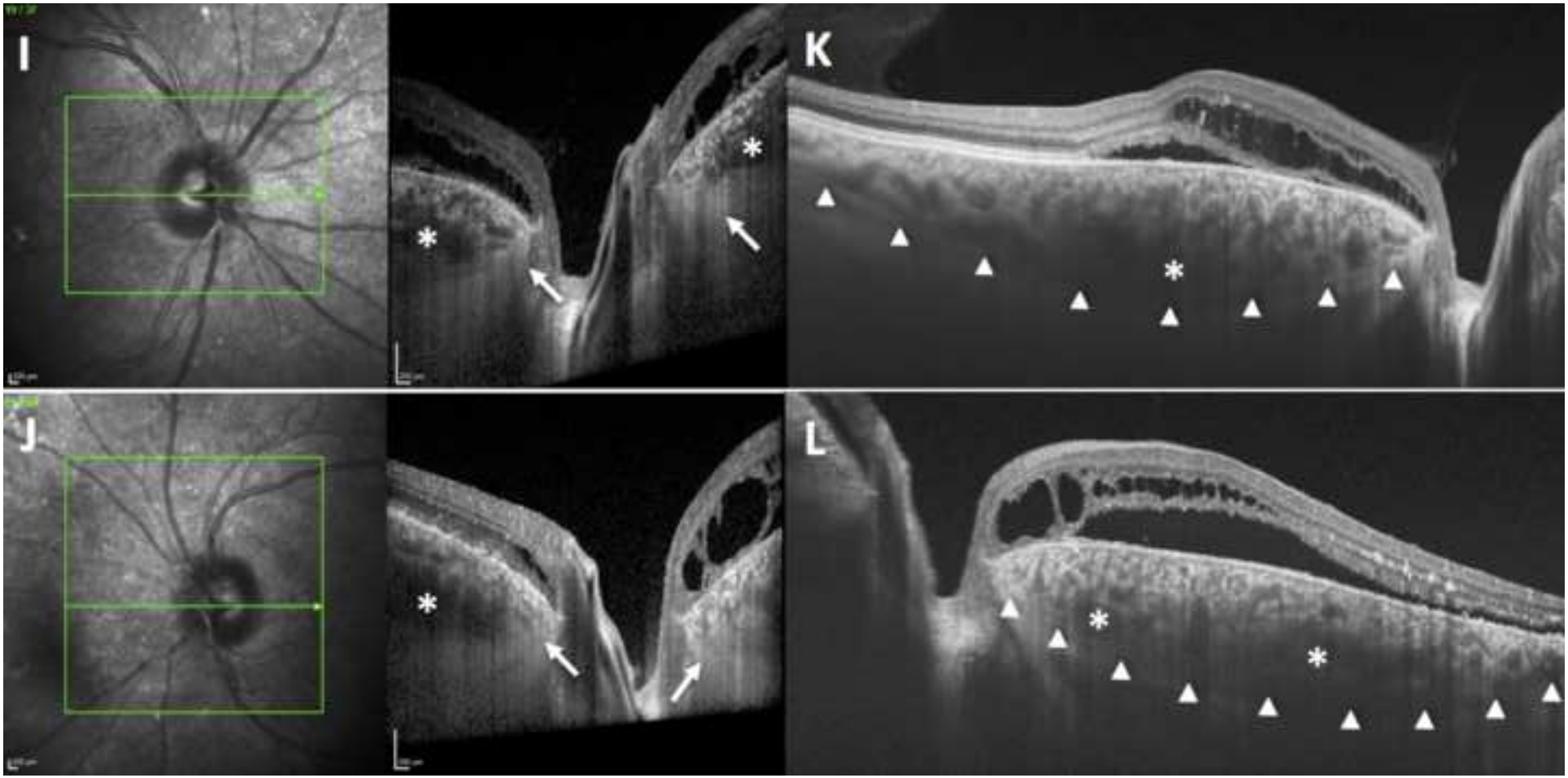

Fig 3

Click here to download Figure (Please type in the figure number in the Description Box; Fig 1, Fig 2, etc.) Figure 3.tiff

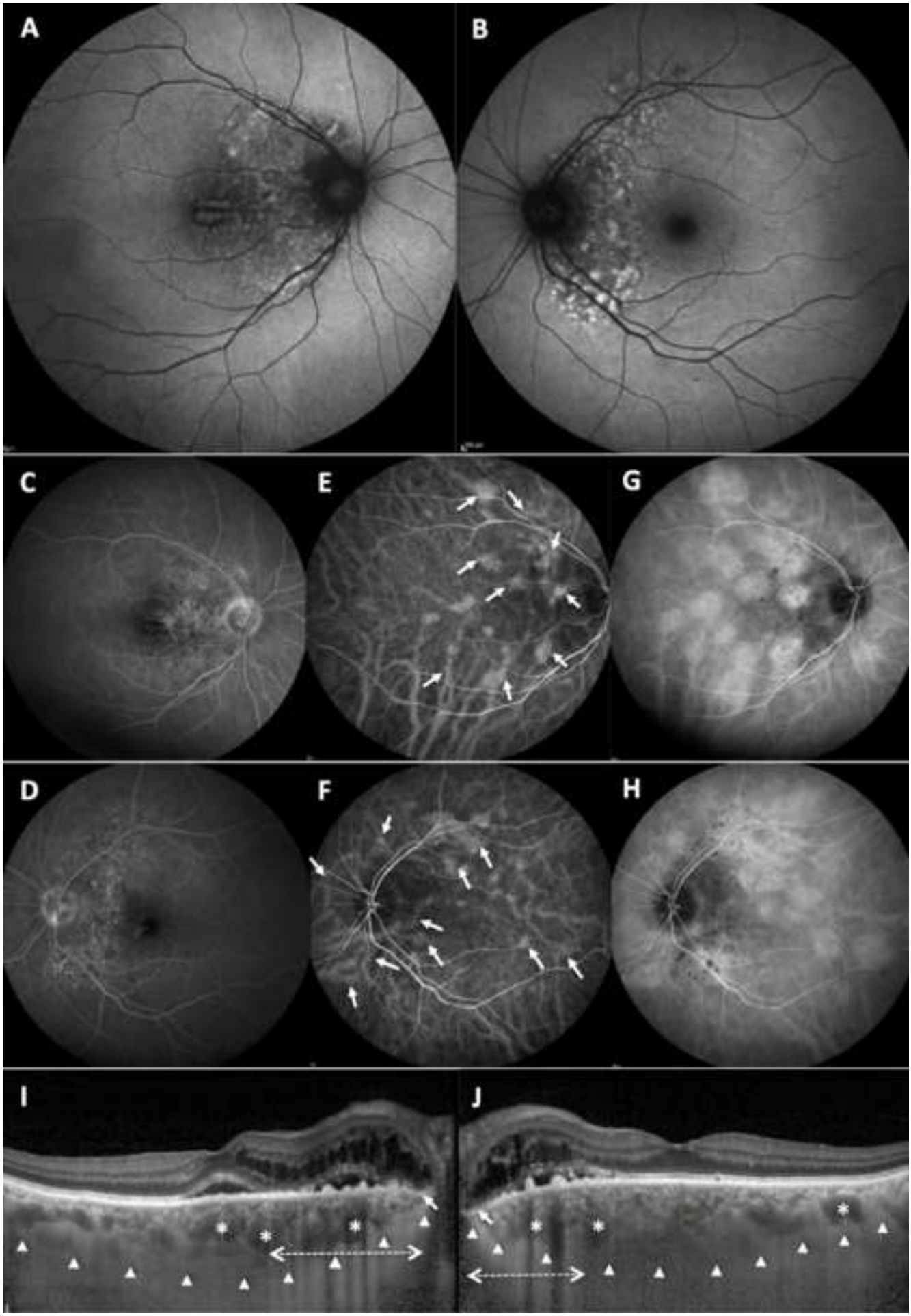

Fig 4

Click here to download Figure (Please type in the figure number in the Description Box; Fig 1, Fig 2, etc.) Figure 4.tiff

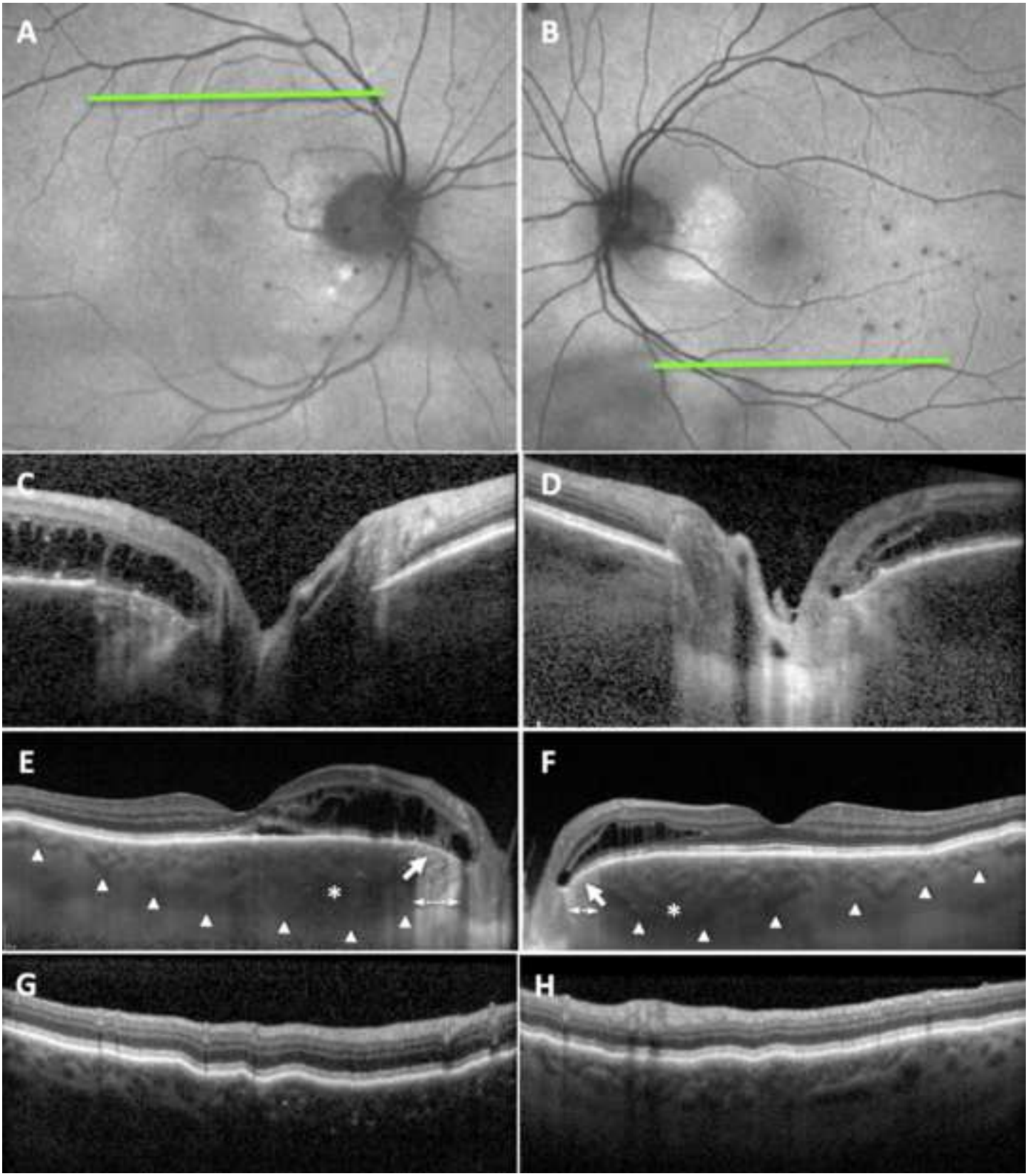

Fig 5

Click here to download Figure (Please type in the figure number in the Description Box; Fig 1, Fig 2, etc.) Figure 5.tiff

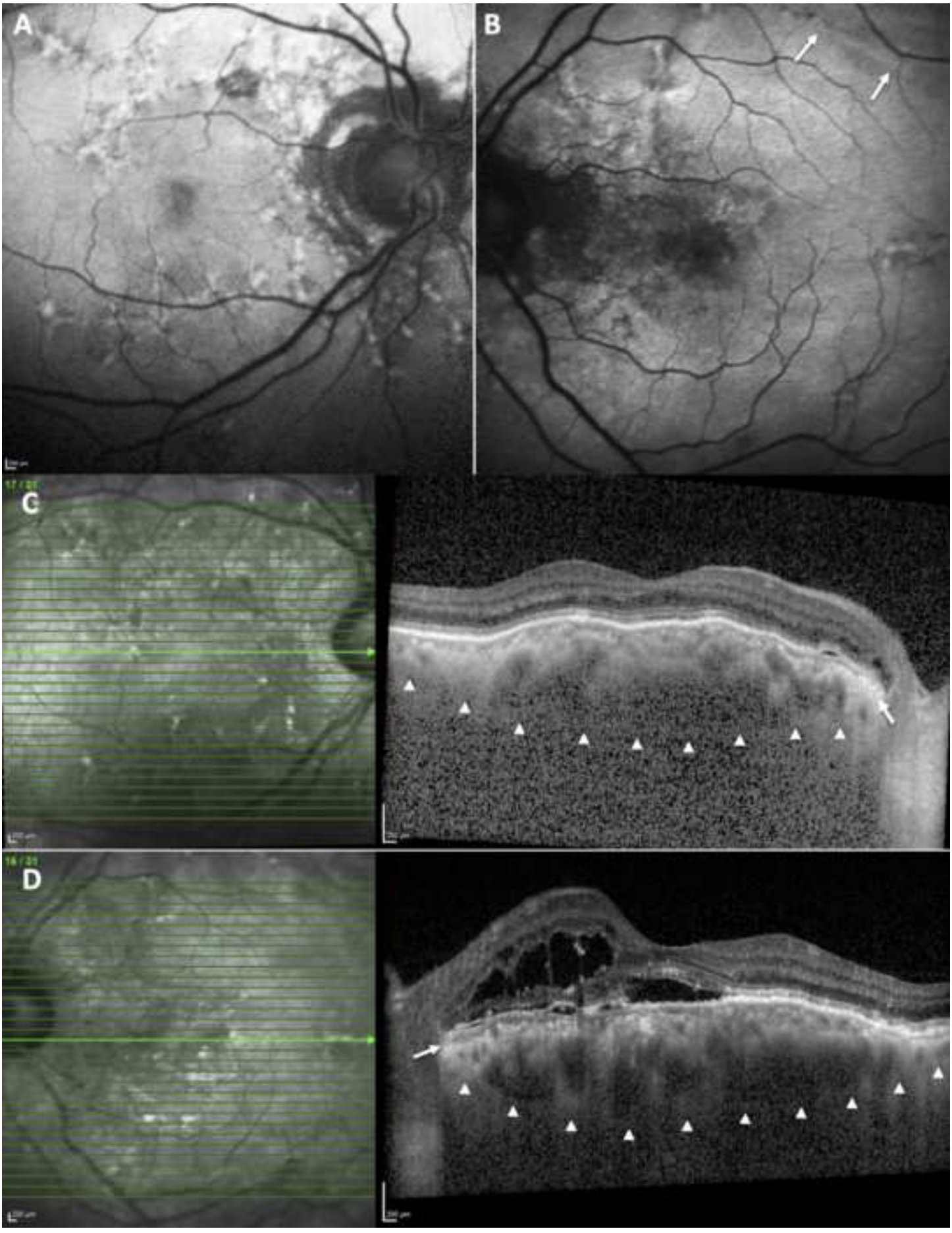

Fig 6

Click here to download Figure (Please type in the figure number in the Description Box; Fig 1, Fig 2, etc.) Figure 6.tiff

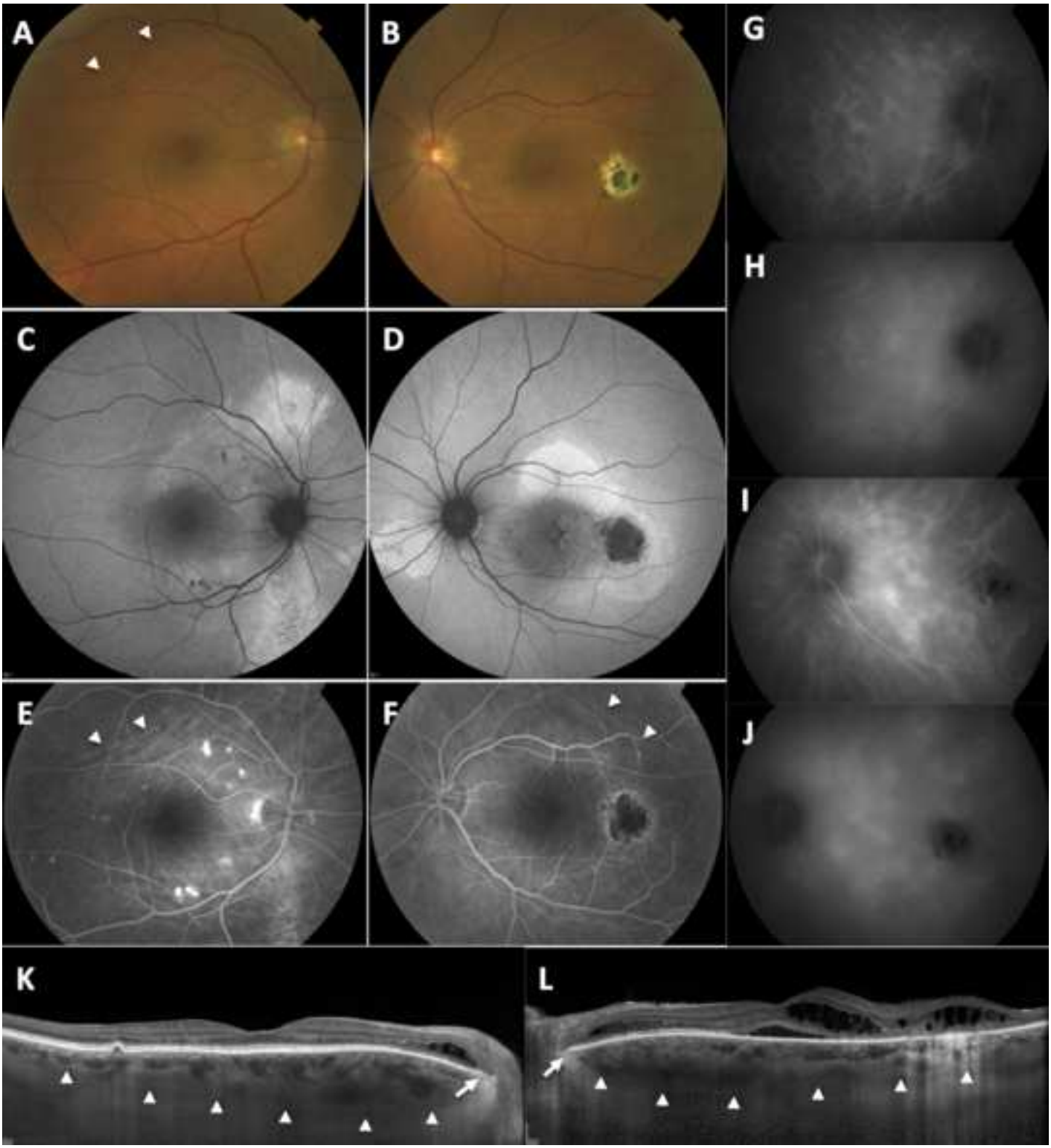

Fig 7

Click here to download Figure (Please type in the figure number in the Description Box; Fig 1, Fig 2, etc.) Figure 7.tiff

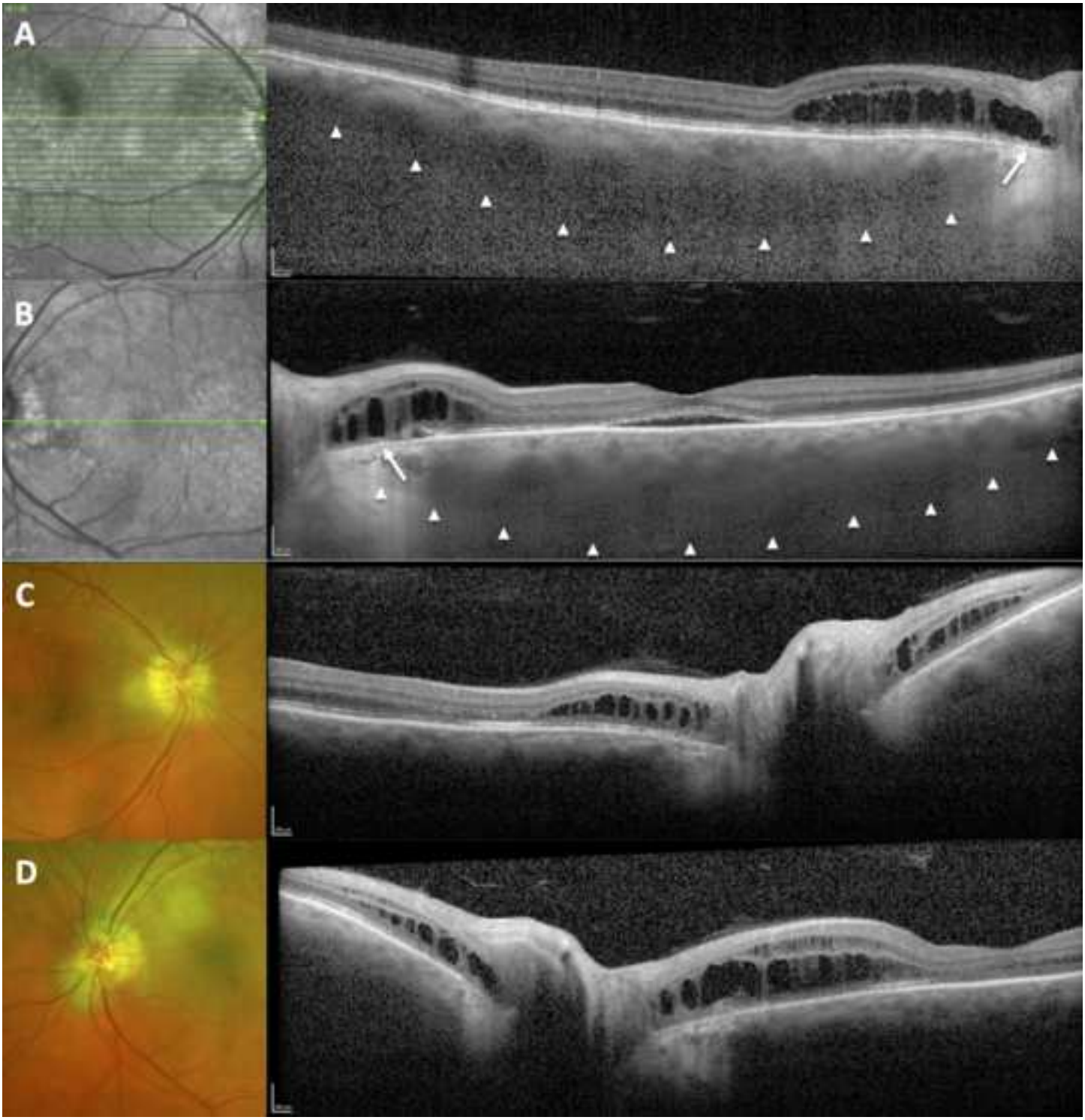

Fig 8

Click here to download Figure (Please type in the figure number in the Description Box; Fig 1, Fig 2, etc.) Figure 8.tiff

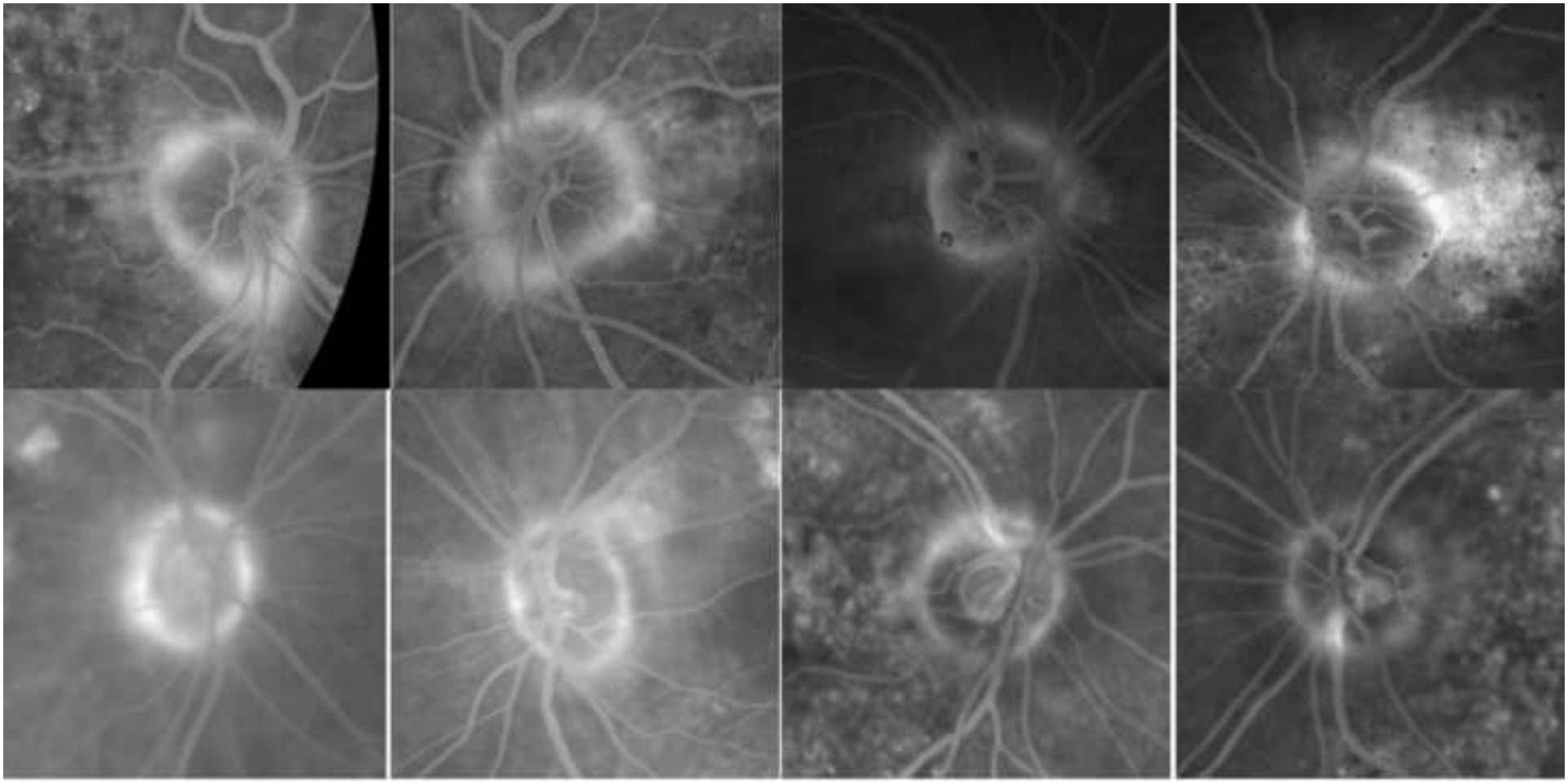

Fig 9

Click here to download Figure (Please type in the figure number in the Description Box; Fig 1, Fig 2, etc.) Figure 9.tiff

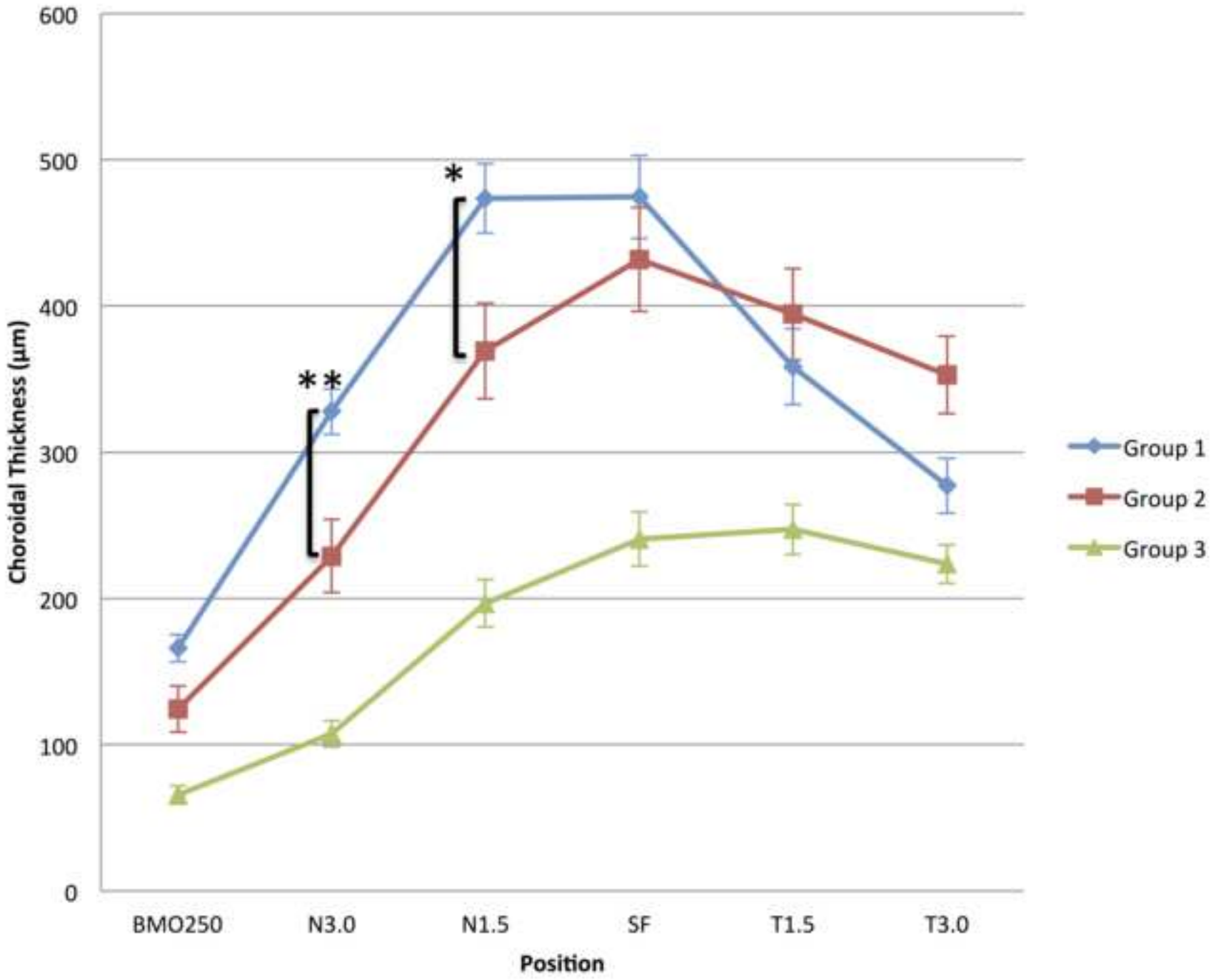

Fig 10

Click here to download Figure (Please type in the figure number in the Description Box; Fig 1, Fig 2, etc.) Figure 10.tiff

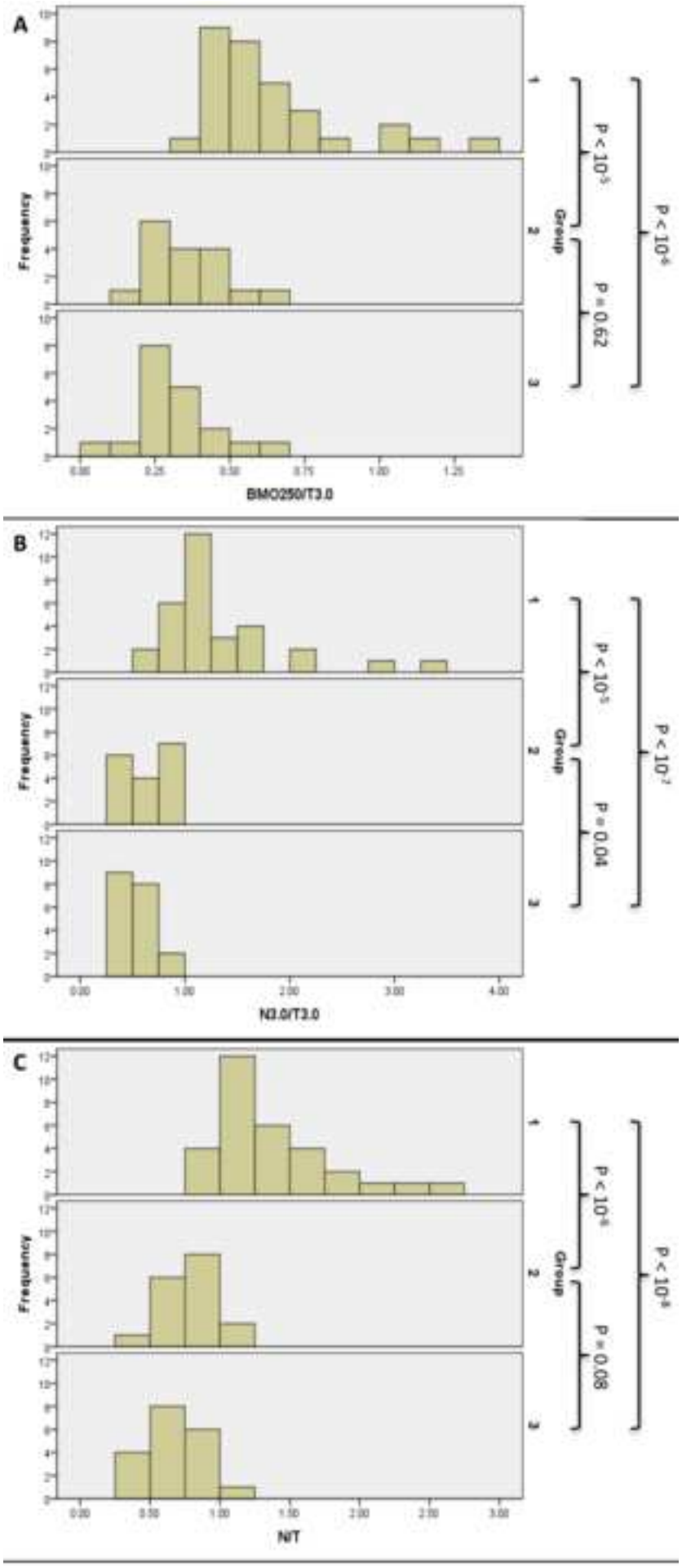

Table 1. Demographic and clinical data of patients with peripapillary pachychoroid syndrome.

Patient	Age (years)	Sex	Eye	VA	Axial Length (mm)	Spherical Equivalence	Choroidal Folds	Cup to Disc Ratio	Underlying Diseases
1	65	F	OD	20/50	23.8	+6.50	Present	0.4	Monoclonal gammopathy of uncertain significance, Reynaud's disease,
			OS	20/30	23.7	+5.75	Present	0.4	Chairi I malformation
2	86	F	OD	20/30	21.9	NA	Present	0.2	Hypertension, Hypercholesterol, sick sinus syndrome, breast cancer
			OS	20/60	21.8	NA	Present	0.3	status post mastectomy and radiation
3	75	M	OD	20/40	23.7	+2.00	Present	0.2	Hypertension, sleep apnea
			OS	20/25	23.5	+2.00	Present	0.3	
4	71	M	OD	20/20	23.1	`+3.75	Present	0.1, edema	Hyperlipidemia, prostrate cancer (inactive), transient ischemic attack,
			OS	20/40	22.8	+4.125	Present	0.1, edema	anxiety
5	69	M	OD	20/25	23.6	-0.75	Present	0.2	Diabetes mellitus type 2
			OS	20/25	23.8	-0.75	Present	0.3	
6	70	M	OD	20/50	22.6	+2.00	Present	0.2, edema	Multiple myeloma
			OS	20/25	22.1	+2.50	Present	0.3, edema	
7	79	M	OD	20/20	24.6	NA	Absent	0.3	None
			OS	20/30	24.4	NA	Absent	0.3	
8	73	F	OD	20/25	NA	NA	Present	0.1	Hypertension, melanoma of foot and leg, Raynaud’s disease,
			OS	20/40	NA	NA	Present	0.1	osteoarthritis, osteopenia

9	63	M	OD	20/40	20.0	NA	Present	0.3	Hypertension
			OS	20/120	20.0	NA	Present	0.3	
10	67	M	OD	20/25	NA	+4.50	Present	0.4	Kidney failure with renal artery stenosis, non invasive bladder tumors
			OS	20/30	NA	NA	Present	0.4	
11	73	M	OD	20/20	NA	NA	Absent	0.1	End-stage renal disease status post kidney transplantation, coronary
			OS	20/60	NA	NA	Absent	0.1	artery disease, diabetes mellitus, hypertension, hyperlipidemia
12	75	M	OD	20/25	NA	NA	Present	0.1	Diabetes mellitus, hypertension, hyperlipidemia, sleep apnea, coronary
			OS	20/30	NA	NA	Present	0.1	artery disease, anemia, pancreatic cyst, chronic renal insufficiency
13	70	M	OD	20/80	23.8	+1.25	Present	0.1	Hypertension, hyperlipidemia
			OS	20/25	23.9	+0.50	Present	0.1	
14	82	M	OD	20/25	NA	NA	Present	0.25	Chronic kidney disease, polymyalgia rheumatica (on prednisolone)
			OS	20/25	NA	NA	Present	0.2	
15	65	M	OD	20/250	NA	NA	Absent	0.2	Diabetes mellitus type 2
			OS	20/30	NA	NA	Absent	0.3	
16	58	M	OD	20/25	NA	+2.00	Absent	0.2	None

Table 2. Demographic data of the 3 groups of subjects in this study.

	Group 1 (PPS)	Group 2 (PDS)	Group 3 (Normal)	P-values
Age (years)				
Mean ± SD	71.3 ± 7.2	63.7 ± 9.7	69.3 ± 5.7	0.1170
Range	58-86	52-80	61-79	
Sex (male/female, %male)	13/3, 81%	9/2, 82%	4/8, 33%	0.0180
LogMAR VA (mean ± SD)	0.2 ± 0.2	0.3 ± 0.5	0.0 ± 0.1	0.0004
Mean Snellen VA	20/32	20/40	20/20	

LogMAR, logarithm of the minimum angle of resolution; PPS, peripapillary pachychoroid syndrome; PDS, pachychoroid disease spectrum; SD, standard deviation; VA, visual acuity